Integrated Damage Mechanics Approach to Brittle and Ductile Crack Propagation

Geralf Hütter[1,*], Thomas Linse[2], Uwe Mühlich[1], Meinhard Kuna[1]

[1] Institute of Mechanics and Fluid Dynamics, TU Bergakademie Freiberg, 09596 Freiberg, Germany
[2] Institute of Solid Mechanics, TU Dresden, 01062 Dresden, Germany
* Corresponding author: Geralf.Huetter@imfd.tu-freiberg.de

Abstract With decreasing temperature the failure of typical engineering metals changes from ductile fracture to cleavage. A possible cleavage initiation in the brittle-ductile transition region is typically evaluated by stress-based criteria like those after Ritchie-Knott-Rice or of Weibull-type. Such models describe the experimental results adequately in the lower brittle-ductile transition region but problems arise in the upper part of the transition region.
In the present study cleavage is modeled by a cohesive zone and ductile damage is described by a non-local Gurson-model. With this modeling of both failure mechanisms the fracture initiation and propagation can be simulated in the whole brittle transition region. The results show that the crack tip constraint has a considerable influence on the stability of the crack propagation.
Keywords fracture mechanics, brittle-ductile transition, non-local Gurson model, FEM simulation

1. Introduction

In the range of room temperature typical engineering metals fail by a ductile mechanism. Thereby, the voids nucleated at non-metallic inclusions grow and coalesce finally to a macroscopic crack. Due to the plastic deformations much energy is dissipated with this mechanism leading to a high macroscopic fracture toughness. In contrast, at low temperatures fracture by cleavage occurs at favorably oriented crystallographic planes in the particular grains. With this mechanism considerably less energy is dissipated compared to the ductile mechanism which is why the macroscopic material behavior is termed as brittle. In the ductile-brittle transition region both mechanisms are observed, see Fig. 1. In this regime a large scatter of the fracture toughness values is observed for specimens of nominally identical material. This behavior is caused by the strong sensitivity to local material imperfections.

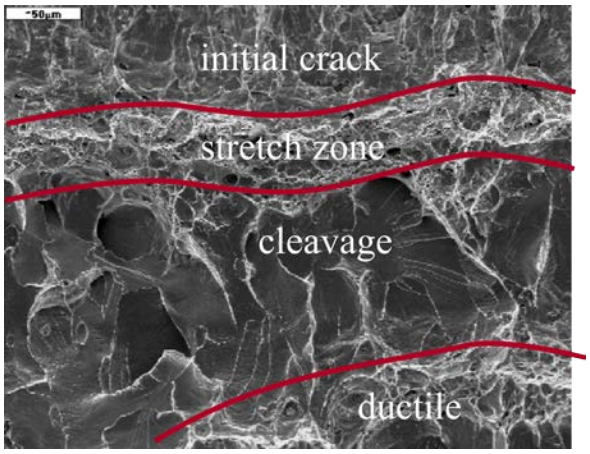

Fig. 1: Ductile-brittle fracture surface [1]

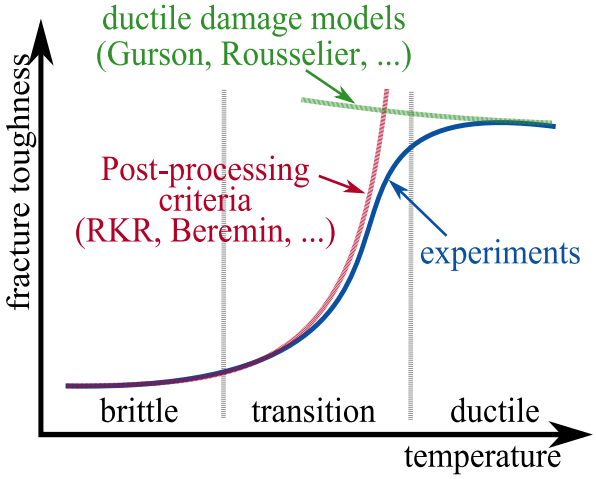

Fig. 2: Models for brittle-ductile transition

Due to the relevance in engineering applications numerous approaches were developed to describe the behavior in the ductile-brittle transition region. Mostly, the ductile mechanism is incorporated

by damage models like those after Gurson or Rousselier or modifications thereof. With such models all stages of crack initiation and propagation can be simulated. In contrast, cleavage is typically associated with unstable crack propagation. For this reason a possible cleavage initiation is usually evaluated by stress-based criteria like those after Ritchie-Knott-Rice (RKR) [2] or Beremin [3]. Especially the Beremin model and its numerous modifications enjoy great popularity as those models are probabilistic and the prediction of failure probabilities corresponds to the experimentally observed large scatter of measured fracture toughness values. The failure probabilities rely on the so-called weakest-link theory where the failure of an element is assumed to coincide with the failure of the complete structure.
Comparisons with experiments show that models of Beremin-type allow realistic predictions in the lower ductile-brittle transition region. However, problems arise in the upper ductile-brittle transition region even if the ductile crack propagation is incorporated as sketched in Fig. 2. Furthermore, the weakest-link theory predicts a vanishing survival probability of very large specimens at arbitrary small loadings. Anderson, Stienstra and Dodds [4] argue that this prediction is physically questionable since some work is always necessary to separate the crystallographic planes. Experiments confirm the existence of a corresponding lower-bound fracture toughness, see e.g. [5]. The problem of models of Beremin-type is the identification of cleavage initiation with immediate unstable crack propagation since the stability of crack propagation is in general a matter of the interaction of material properties, specimen type, specimen size and loading.
In the present study cleavage is modeled by a cohesive zone and ductile damage is described by a non-local Gurson-model. With this modeling of both failure mechanisms the fracture initiation and propagation can be simulated in the whole brittle transition region. The stability is an outcome of the simulations.

2. Model

Concretely, cleavage is modeled by a so-called cohesive zone. In a model of this kind it is assumed that the normal stress $\sigma(x)$ transmitted at each point x in the process zone depends on the local separation $\delta(x)$ of the crack edges as sketched in Fig. 3. The particular relation between σ and δ is described by the cohesive law. In the present study the exponential law after Xu and Needleman [6] is employed. The maximum transmittable stress σ_c is termed as cohesive strength. The area Γ_0 is the work of separation and corresponds to the work which is necessary for the formation of new surfaces. Correspondingly, Γ_0 has the unit of work per area.

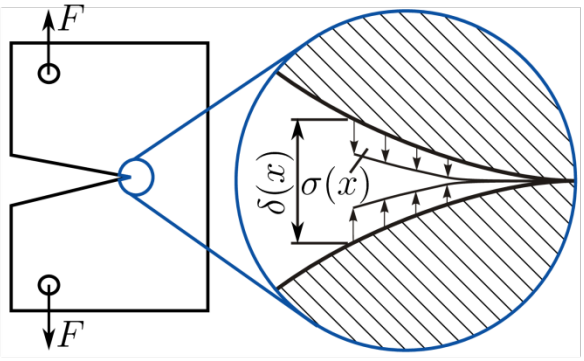

Fig. 3: Cohesive zone at the crack tip

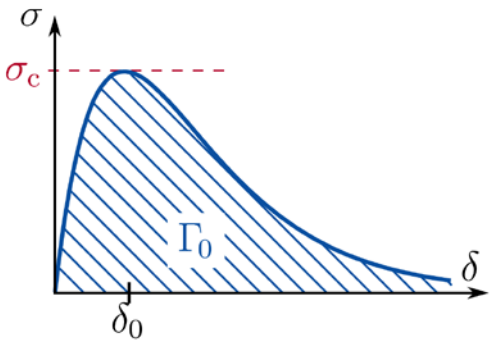

Fig. 4: Exponential cohesive law

Modeling cleavage by means of a cohesive zone captures phenomenologically two essential

experimentally observed issues. Firstly, the softening initiates (in the considered case of mode-I loading) if the maximum principal stress in the ligament reaches the value σ_c. Secondly, Γ_0 is the minimum work necessary for the formation of free surface in absence of plastic deformations and corresponds thus to the lower-bound fracture toughness. In finite-element models implementing a cohesive zone, the results are expected to converge with an increasing mesh resolution.

In the bulk material embedding the cohesive zone the ductile damage mechanism is described by the Gurson-model [7] in the established modification by Tvergaard und Needleman [8] (GTN-model). However, from this approach (and all other classical damage models) it is known that the results depend strongly on the element size and orientation. But for a consistent numerical implementation of the cohesive zone the stresses around the crack tip need to be resolved very fine. In order to overcome this problem the non-local extension of the GTN-model by Linse et al. [9] is employed for the following simulations. In classical constitutive theories the softening at a material point depends only on the internal state variables at this point. Within a non-local approach a region of finite size around the particular material point is incorporated for the softening. The dimension of this region is associated with a relevant microstructural length of the damage mechanism, for the ductile mechanism thus to the mean distance of the voids.

Concretely, in the non-local modification by Linse et al. the flow potential

$$\Phi = \frac{\sigma_{\mathrm{eq}}^2}{\sigma_{\mathrm{M}}^2} + 2q_1 f^* \cosh\left(\frac{3q_2}{2}\cdot\frac{\sigma_{\mathrm{h}}}{\sigma_{\mathrm{M}}}\right) - 1 - \left(q_1 f^*\right)^2 \tag{1}$$

of the original GTN-model is retained. Therein, σ_{eq} and σ_{h} denote the Mises stress and the hydrostatic stress, σ_{M} is the equivalent yield stress of the matrix material and q_1 and q_2 are the fitting parameters after Tvergaard und Needleman. In the following the established values q_1=1.5 and q_2=1 are assigned. In the initial stage the effective void volume fraction f* corresponds to the actual value f. In the stage of void coalescence which initiates at $f = f_c$, the effective value f* increases faster than f by the factor K:

$$f^* = \begin{cases} f & f \le f_c \\ f_c + (f - f_c)K & f_c < f \le f_f \end{cases} \quad \text{with} \quad K = \frac{f_u - f_c}{f_f - f_c}, \quad f_u = \frac{1}{q_1} \tag{2}$$

At $f = f_f$ (corresponding to $f^*=f_u$) the material has lost its load carrying capacity completely. The non-local modification concerns the evolution law of f. In contrast to the classical GTN-model the non-local plastic volumetric strain $\varepsilon_{\mathrm{nl}}$ is used in this law:

$$\dot{f} = (1 - f)\dot{\varepsilon}_{\mathrm{nl}} + \dot{f}_{\mathrm{N}} \tag{3}$$

The nucleation term f_{N} is not considered in the following for simplicity, but all voids are assumed to be initially present and are thus captured with the initial void volume fraction f_0. The non-local plastic volumetric strain $\varepsilon_{\mathrm{nl}}$ is defined in a so-called implicit-gradient formulation by an additional partial differential equation of Helmholtz-type

$$\varepsilon_{\mathrm{nl}} + l_{\mathrm{nl}}^2 \Delta\varepsilon_{\mathrm{nl}} = \varepsilon_v \tag{4}$$

wherein the local volumetric plastic strain ε_{v} forms the source term. A region around the current material point is incorporated through the Laplace-operator Δ. The intrinsic length scale l_{nl} enters as

the weighting prefactor of the Laplace-operator. Regarding the boundary conditions necessary in addition to the Helmholtz-equation the reader is referred to [9,10]. A one-parametric power-law is implemented for the matrix yield stress σ_M in such a way that in a uniaxial tension test with the compact material f=0 a relation

$$\sigma = \sigma_y \left(\frac{E\varepsilon}{\sigma_y} \right)^N \tag{5}$$

between true stress σ and logarithmic strain ε is obtained. Therein, E denotes Young's modulus and σ_y and N are the initial yield stress and the hardening exponent, respectively. The following simulations are performed with σ_y/E=0.003 and N=0.1 and a Poisson ratio of ν=0.3 corresponding to typical medium strength engineering alloys (e.g. E=210 GPa, σ_y=500…700 MPa). The initial void volume fraction is assumed to be f_0=0.01. The work of separation is taken as Γ_0=1/3 $\sigma_y l_{nl}$ which is realistic for the material which will be considered finally for a comparison between simulations and experiments.

Due to the non-local formulation the boundary-value problem is well-posed also in the case of ductile softening. Thus, the combined model of cohesive zone and non-local GTN-model leads to a mesh-independent solution in the complete temperature range. Correspondingly, the local field quantities in the process zone are determined only through the material parameters and the loading. In particular, the size of the process zone is defined by the material parameters of unit length. For ductile failure this is the non-local length l_{nl} whereas for cleavage the size of the process zone is related to the characteristic cohesive separation δ_0 which is necessary to reach the cohesive strength σ_c. For the employed cohesive law this value amounts to $\delta_0=\Gamma_0/(\sigma_c \exp(1))$, compare Fig. 4. For the simulation of the crack propagation by means of the finite element method (FEM) the fields in the process zone need to be resolved sufficiently fine. For realistic values, δ_0 is always smaller than l_{nl} so that the maximum feasible element size is determined by δ_0. According to a performed convergence study elements of edge length b_e=1.2 δ_0…1.8 δ_0 are placed at the ligament. A typical mesh at the crack tip is depicted in Fig. 5. Only a half-model needs to be meshed for symmetry reasons. The cohesive elements do not have a geometric thickness and are thus only sketched in the figure.

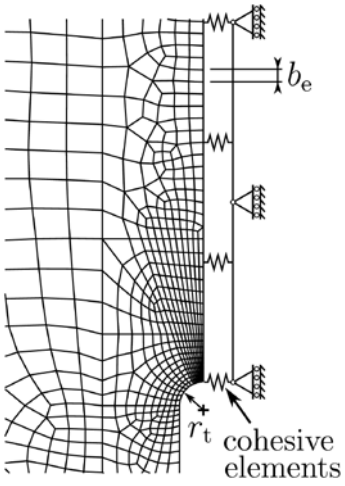

Fig. 5: FE-mesh at the crack tip

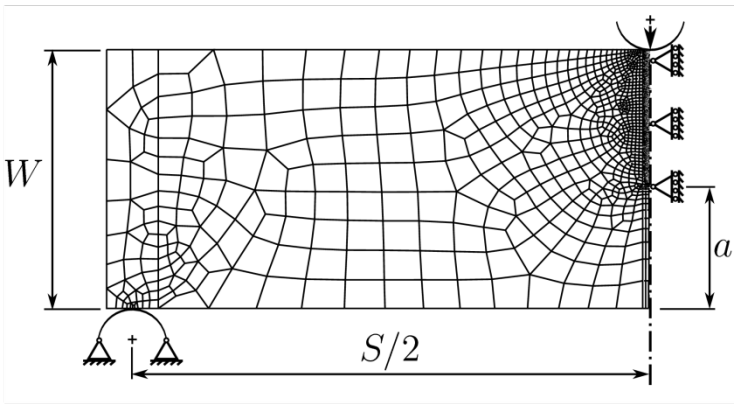

Fig. 6: FE-mesh for 3PB specimen

Realistically, an initial stage of crack tip blunting is expected to occur with the non-local GTN-model before the fracture initiation [9,10]. In order to handle the associated strain singularity an initial radius r_t is introduced in the FE-model. The radius r_t has to be small compared to l_{nl} preventing an inadmissible perturbance of the solution. The mesh in Fig. 5 fulfills this requirement.
For the computations the commercial FE-code Abaqus/standard is employed. Dynamic simulations are performed with implicit time integration under plane-strain conditions. The loading is applied quasi-statically. The elements for non-local GTN-model and the cohesive elements are both implemented with quadratic shape functions as user-defined elements via the UEL-interface. The crack propagation is simulated in the following for a three-point bending specimen (Fig. 6) or under a K_I-dominated far-field (boundary-layer model, see [10]).

3. Results

First, the influence of the cohesive strength σ_c is investigated. In order to exclude possible effects of the geometry of a particular specimen, the limit case of a K_I-dominated far-field is considered. A dimensional analysis shows that under these conditions the ratio of σ_c and initial yield stress σ_y is the only relevant parameter. In metals σ_y increases with decreasing temperature. If σ_c is assumed to be independent of the temperature, σ_c/σ_y increases with increasing temperature.
Computed crack growth resistance curves (R-curves) are shown in Fig. 7 for several values of σ_c/σ_y. In addition, the active damage mechanism is marked. It has to be noticed that the crack growth resistance J_R is normalized with respect to the yield stress σ_y and the non-local length l_{nl}. The amount of crack growth Δa is normalized by l_{nl} as well. The results show that the crack growth resistance increases with the ratio σ_c/σ_y, i.e. with increasing temperature. For σ_c/σ_y=2.6 the crack growth resistance is determined by the work of separations Γ_0. In the lower ductile-brittle transition

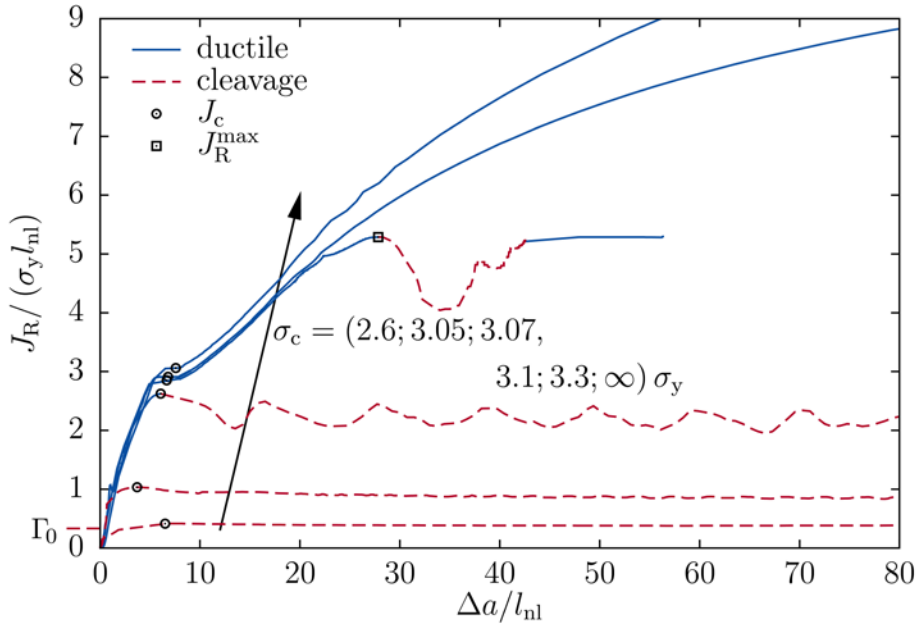

Fig. 7: Crack growth resistance curves

region at σ_c/σ_y=3.05 there is still pure cleavage but already a considerably higher crack growth resistance J_R. The difference between J_R and Γ_0 is caused by the dissipation due to the plastic

deformations during the blunting of the crack tip. After the fracture initiation at $J_R=J_c$ the plastic dissipation decreases leading to a decaying R-curve. For a prescribed loading $J=J_c$ this point is unstable so that a dynamic crack propagation initiates. For σ_c/σ_y=3.07 and σ_c/σ_y=3.10 the crack begins to propagate with the ductile mechanism until cleavage initiates and the propagation becomes dynamic, too. The distribution of the void growth behind the current crack tip is depicted in Fig. 8 showing a so-called stretch zone. Whilst the crack propagates only by cleavage for σ_c/σ_y=3.07, the crack arrests again for σ_c/σ_y=3.10 followed by ductile propagation. Such a behavior accords to experimental results, compare Fig. 1.

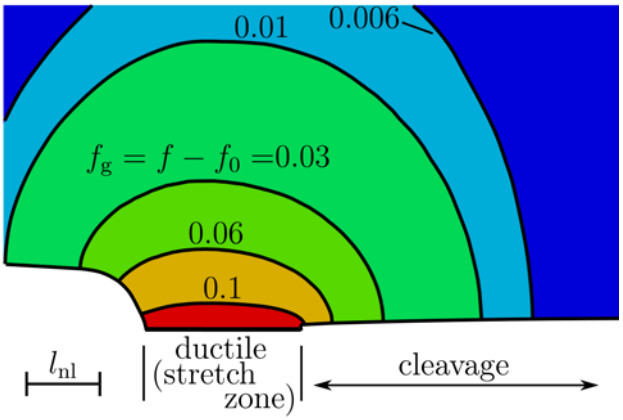

Fig. 8: Stretch zone at initial crack tip (σ_c/σ_y=3.07)

In order to investigate the effect of the crack tip constraint, now the crack propagation in a shallow-crack three-point bending specimen of width W=100 l_{nl} is simulated with a FE-mesh like that in Fig. 6. The relative crack depth amounts to a/W=0.15, a value corresponding to the experimental data which will be used below for a comparison. The computed R-curves are depicted in Fig. 9 for the lower ductile-brittle transition region.

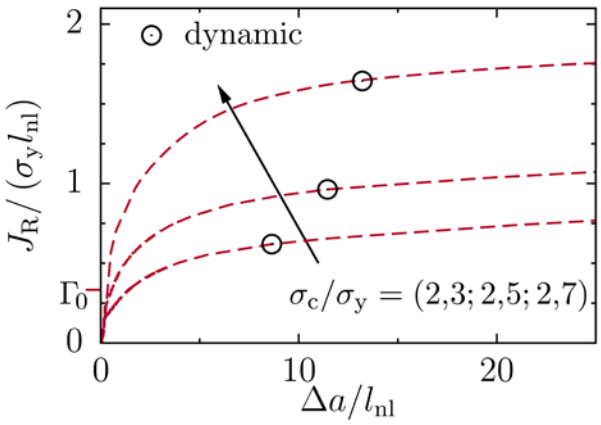

Fig. 9: R-curves for shallow-cracked specimen (a/W=0.15)

The results show that initially the crack grows by cleavage but nevertheless stably until the crack propagation becomes dynamic at the unstable point. Typically, in the context of brittle damage this point is used for the definition of the fracture toughness J_c. However, because of the initially stable crack propagation a J_c defined this way does not depend only on the crack tip constraint at the initial crack tip. Merely, it is also significantly influenced by the evolution of the crack tip constraint with ongoing crack growth.

In order to verify the presented model the simulation results are compared to the experimental data of Sorem, Dodds und Rolfe [11] in the following. These authors investigated the fracture behavior of an A36 steel in the ductile-brittle transition region. They focused on the effect of the crack-tip constraint which is why specimens of different crack depth were employed having all a width of W=34 mm. Since the predictive capabilities of the presented model shall be checked the model parameters are determined only from the deep-cracked standard specimen with a/W=0.50. Finally, the behavior of the shallow-cracked specimen with a/W=0.15 is simulated.

According to the procedure proposed in [10] the intrinsic length of the non-local GTN-model is determined to be l_{nl}=0.34 mm corresponding to a size ratio of W/l_{nl} = 93.5. The yield stress is given in [11] for the complete temperature range. The work of separation corresponds to the lower-bound fracture toughness as discussed above and is assumed to be temperature-independent for simplicity leading to a value Γ_0=0.028 MPam. The cohesive strength is now determined via the ductile-brittle transition temperature which gives σ_c=780 MPa.

The fracture toughness values extracted from the simulations of the shallow-cracked specimens (a/W=0.15) are compared to the corresponding experimental data in Fig. 10. It has to be noted that the simulation results from above with W/l_{nl} = 100 are used for convenience. Fig. 10 shows that the shift of the ductile-brittle transition temperature is predicted adequately. Furthermore, it is predicted correctly that even at a high level of fracture toughness of about J_c=0.15 MPam there is pure cleavage. This high fracture toughness is attributed to the initially stable crack propagation by cleavage as found above.

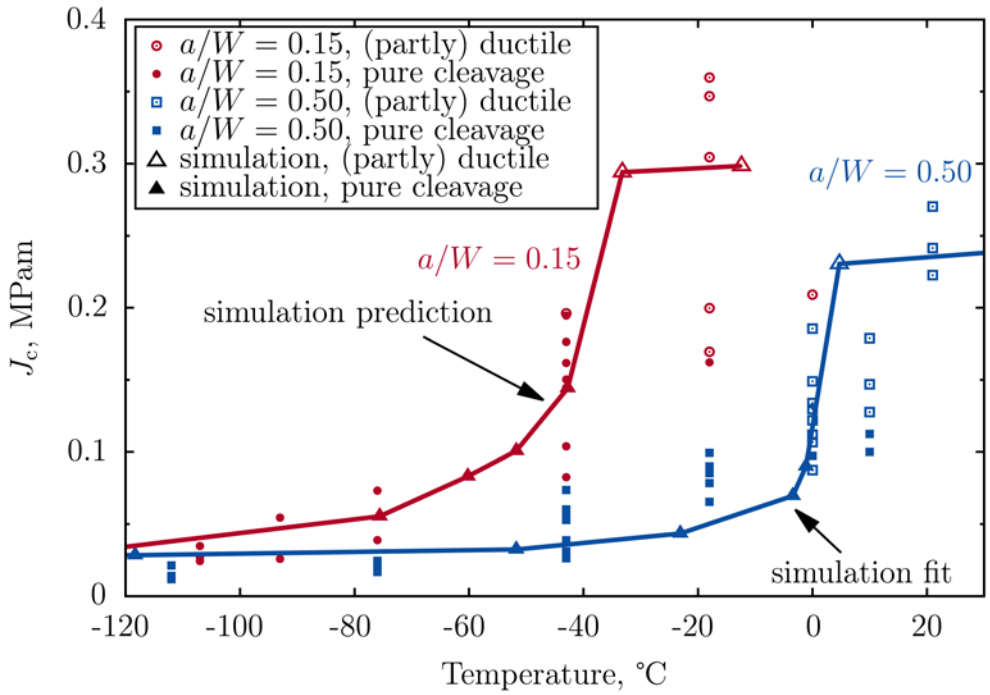

Fig. 10: Fracture toughness of an A36-steel [11] in comparison to simulation results

The employed model is deterministic. Thus, in the current state only mean properties can be considered. It remains open to investigate whether information about the scatter of the fracture toughness values can be gained if local imperfections are considered in the model.

The present contribution is a translation of [13] and outlines the results of [12]. Details of the model, numerical methods, the procedure for the determination of the parameters and the comparison with experimental data can be found in the latter reference.

Acknowledgement

The financial support by the Deutsche Forschungsgemeinschaft (German Research Foundation) under contracts KU 919-14 (Hütter) and INST 267/81-1 FUGG (computing facilities) and by the German Federal Ministry of Economics and Technology under contracts 1501298 and 1501343 (Linse) is gratefully acknowledged. The authors thank Stephan Roth for providing the implementation of the cohesive element for Abaqus.

References

[1] A. Neimitz, J. Galkiewicz and I. Dzioba, The ductile-to-cleavage transition in ferritic Cr-Mo-V steel: A detailed microscopic and numerical analysis, Eng. Fract. Mech., 77(2010), 2504-2526.
[2] R. Ritchie, J. Knott and J. Rice, On the relationship between critical tensile stress and fracture toughness in mild steel, J. Mech. Phys. Solids, 21(1973), 395-410.
[3] F. M. Beremin, A Local Criterion for Cleavage Fracture of a Nuclear Pressure Vessel Steel, Metall. Mater. Trans. A., 14(1983), 2277-2287.
[4] T. Anderson, D. Stienstra and R. Dodds Jr, A Theoretical Framework for Addressing Fracture in the Ductile-Brittle Transition Region, ASTM STP 1207 (1994), 186-214.
[5] J. Heerens and D. Hellmann, Development of the Euro fracture toughness dataset, Eng. Fract. Mech., 69(2002), 421-449.
[6] X. P. Xu and A. Needleman, Void nucleation by inclusion debonding in a crystal matrix, Model. Simul. Mater. Sc., 1 (1993), 111-132.
[7] A. L. Gurson, Continuum Theory of Ductile Rupture by Void Nucleation and Growth, J. Eng. Mater-T. ASME, 99(1977), 2-15.
[8] V. Tvergaard, Influence of voids on shear band instabilities under plane strain conditions, Int. J. Fracture, 17(1981), 389-407.
[9] T. Linse, G. Hütter and M. Kuna, Simulation of crack propagation using a gradient-enriched ductile damage model based on dilatational strain, Eng. Fract. Mech., 95(2012), 13-28.
[10] G. Hütter, T. Linse, U. Mühlich and M. Kuna, Simulation of Ductile Crack Initiation and Propagation by means of a Non-local GTN-model under Small-Scale Yielding, Int. J. Solids. Struct., 50(2013), 662-671.
[11] W. A. Sorem, R. H. Dodds and S. T. Rolfe, Effects of crack depth on elastic-plastic fracture toughness, Int. J. Fracture, 47(1991), 105-126.
[12] G. Hütter, Multi-Scale Simulation of Crack Propagation in the Ductile-Brittle Transition Region, TU Bergakademie Freiberg, dissertation, in preparation.
[13] G. Hütter, T. Linse, U. Mühlich, T. Linse, Simulation der Rissausbreitung im gesamten spröd-duktilen Übergangsbereich, in: P. Hübner (Ed.), DVM-Bericht 245, 2013, 49-58